

# An extreme climate gradient-induced ecological regionalization in the Upper Cretaceous Western Interior Basin of North America

Landon Burgener<sup>1,†</sup>, Ethan Hyland<sup>1</sup>, Emily Griffith<sup>2</sup>, Helena Mitášová<sup>1</sup>, Lindsay E. Zanno<sup>3,4</sup>, and Terry A. Gates<sup>3,4</sup>

<sup>1</sup>Department of Marine, Earth and Atmospheric Sciences, 2800 Fauvette Drive, Room 1125, Jordan Hall, North Carolina State University, Raleigh, North Carolina 27695, USA

<sup>2</sup>Department of Statistics, North Carolina State University, 5109 SAS Hall, 2311 Stinson Drive, Raleigh, North Carolina 2769, USA

<sup>3</sup>Department of Biological Sciences, 112 Dericuix Place, Room 3510, Thomas Hall, CB 7614, Raleigh, North Carolina 27695-7614, USA, and North Carolina State University, Raleigh, North Carolina 27695, USA

<sup>4</sup>Paleontology, North Carolina Museum of Natural Sciences, 11 West Jones Street, Raleigh, North Carolina 27601, USA

## ABSTRACT

**The Upper Cretaceous Western Interior Basin of North America provides a unique laboratory for constraining the effects of spatial climate patterns on the macroevolution and spatiotemporal distribution of biological communities across geologic timescales. Previous studies suggested that Western Interior Basin terrestrial ecosystems were divided into distinct southern and northern communities, and that this provincialism was maintained by a putative climate barrier at ~50°N paleolatitude; however, this climate barrier hypothesis has yet to be tested. We present mean annual temperature (MAT) spatial interpolations for the Western Interior Basin that confirm the presence of a distinct terrestrial climate barrier in the form of a MAT transition zone between 48°N and 58°N paleolatitude during the final 15 m.y. of the Cretaceous. This transition zone was characterized by steep latitudinal temperature gradients and divided the Western Interior Basin into warm southern and cool northern biomes. Similarity analyses of new compilations of fossil pollen and leaf records from the Western Interior Basin suggest that the biogeographical distribution of primary producers in the Western Interior Basin was heavily influenced by the presence of this temperature transition zone, which in turn may have impacted the distribution of the entire trophic system across western North America.**

## INTRODUCTION

A primary objective of evolutionary biology is linking the macroevolution and spatiotemporal distribution of organisms with abiotic factors across geologic timescales (e.g., Mayr, 1982; Wright, 1982; Jablonski, 2007). Indeed, studies on the evolution of life often invoke spatial and temporal environmental patterns to explain biogeographic trends such as expansion and contraction of biomes (e.g., Lieberman, 2005; Saupe et al., 2014; Arbour et al., 2016), endemism versus cosmopolitanism (e.g., Lamoreux et al., 2006; Jansson, 2003; Sidor et al., 2005), and the extinction or radiation of major lineages (e.g., Pardo et al., 2019; Alroy, 2010; Anderson et al., 2011). Most studies on the relationship between climate and biotic evolution focus on global constraints and drivers that can be tackled with a coarse approach; however, trends observed at the macroscale do not universally translate to local patterns across short time intervals, which may be heavily influenced by local events (Chiarenza et al., 2019; Barrett, 2014). Such data sets are challenging to assemble due to the unavailability of proportional data on environmental parameters and inherent biases in the preservation of geographically widespread fossil assemblages within geologically short time intervals (Chiarenza et al., 2019; Dean et al., 2020). The vertebrate fossil record of the Upper Cretaceous Western Interior Basin of North America is an exception, as it represents one of the most spatiotemporally contiguous records of Mesozoic vertebrates globally (Gates et al., 2010), providing an opportunity to study fine-scale interactions between climate, tectonic, and biologic systems.

Much research has attempted to link the tectonic and environmental evolution of the Western Interior Basin with perceived paleobiogeographic patterns of terrestrial ecosystems. The hypothesis that Campanian (83.6–72.1 Ma) and

Maastrichtian (72.1–66 Ma) vertebrate assemblages of the Western Interior Basin (especially dinosaurs) were endemic to distinct northern and southern communities originated in the 1970s (Sloan, 1970, 1976; Lehman, 1987; Wolfe and Upchurch, 1987). Attempts to explain the potential presence of distinct biomes within the Western Interior Basin have been the subject of intensifying research since that time (e.g., Lehman, 2001; Sampson and Loewen, 2005; Lehman et al., 2006; Gates et al., 2010, 2012; Sampson et al., 2010; Loewen et al., 2013; Thomson et al., 2013; Longrich, 2014; Leslie et al., 2018; Sankey, 2008; Nydam et al., 2013). These studies suggest that the evolving physiogeography of the Western Interior Basin, coupled with changing climate during the Late Cretaceous, resulted in periodic physical or ecological barriers to vertebrate movement. Other studies (e.g., Vavrek and Larsson, 2010; Wick and Lehman, 2013; Lucas et al., 2016; Berry, 2018) dispute a hypothesis of Western Interior Basin biomes altogether, typically over concerns regarding sampling biases and/or cladotaxonomic issues (e.g., Williamson, 2000; Longrich, 2014; Lucas et al., 2016; Berry, 2018), asynchronous temporal comparisons (Lucas et al., 2006; Lucas et al., 2016; Fowler, 2017), or lack of perceived evidence for a geologic or climatic barrier (e.g., Wolfe and Upchurch, 1987; Amiot et al., 2004; Longrich, 2014; Upchurch et al., 2015; Lucas et al., 2016; Berry, 2018).

Multiple studies have presented compelling evidence that the movement of vertebrates between northern and southern regions of the Western Interior Basin was not impeded by true physical barriers (e.g., Gates et al., 2012; but see Fowler and Freedman Fowler, 2020, for a contrasting view). However, the hypothesis that the Western Interior Basin was divided into distinct climatic zones divided by an ecological boundary zone centered roughly at the paleolatitude of

Landon Burgener  <http://orcid.org/0000-0002-2542-2985>  
†lkburgen@ncsu.edu

the Wyoming–Colorado border as suggested by Lehman (1987, 1997), Sampson et al. (2010), and Gates et al. (2010, 2012) has not been rigorously tested, despite abundant quantitative paleoclimate and paleoenvironmental reconstructions from the region. Here we create spatially interpolated maps of mean annual temperature (MAT) from new compilations of quantitative temperature reconstructions for three time slices (Figs. 1A–1C): 77.4–74.2 Ma (3.2 m.y., middle to late Campanian), 71–69 Ma (2 m.y., early to late Maastrichtian), and 69–66 Ma (3 m.y., late Maastrichtian) to test the hypothesis that a climate barrier existed

within the Western Interior Basin. On the basis of our reconstructions, we identify the existence and evolving location of a MAT transition zone and explore the geographic factors that contributed to its formation. We employ a Monte Carlo approach to constrain the uncertainty associated with the interpolated MAT maps and to test the statistical significance of the identified MAT transition zones. Finally, we compare these MAT maps to interpolated ecoregion maps and assemblage similarity values created from newly compiled data sets of Western Interior Basin pollen and leaf fossil records (Figs. 1A–1C) to investigate the effect

of spatial climate patterns on primary producer distribution within the Western Interior Basin during the terminal Cretaceous.

## North American Cretaceous Western Interior Basin Geography and Climate

### Paleogeography of the Western Interior Basin

The terrestrial climate and environment of the Western Interior Basin were modulated by the Western Interior Seaway and the North American cordillera (Fig. 1), which bounded the regions to the east and west, respectively.

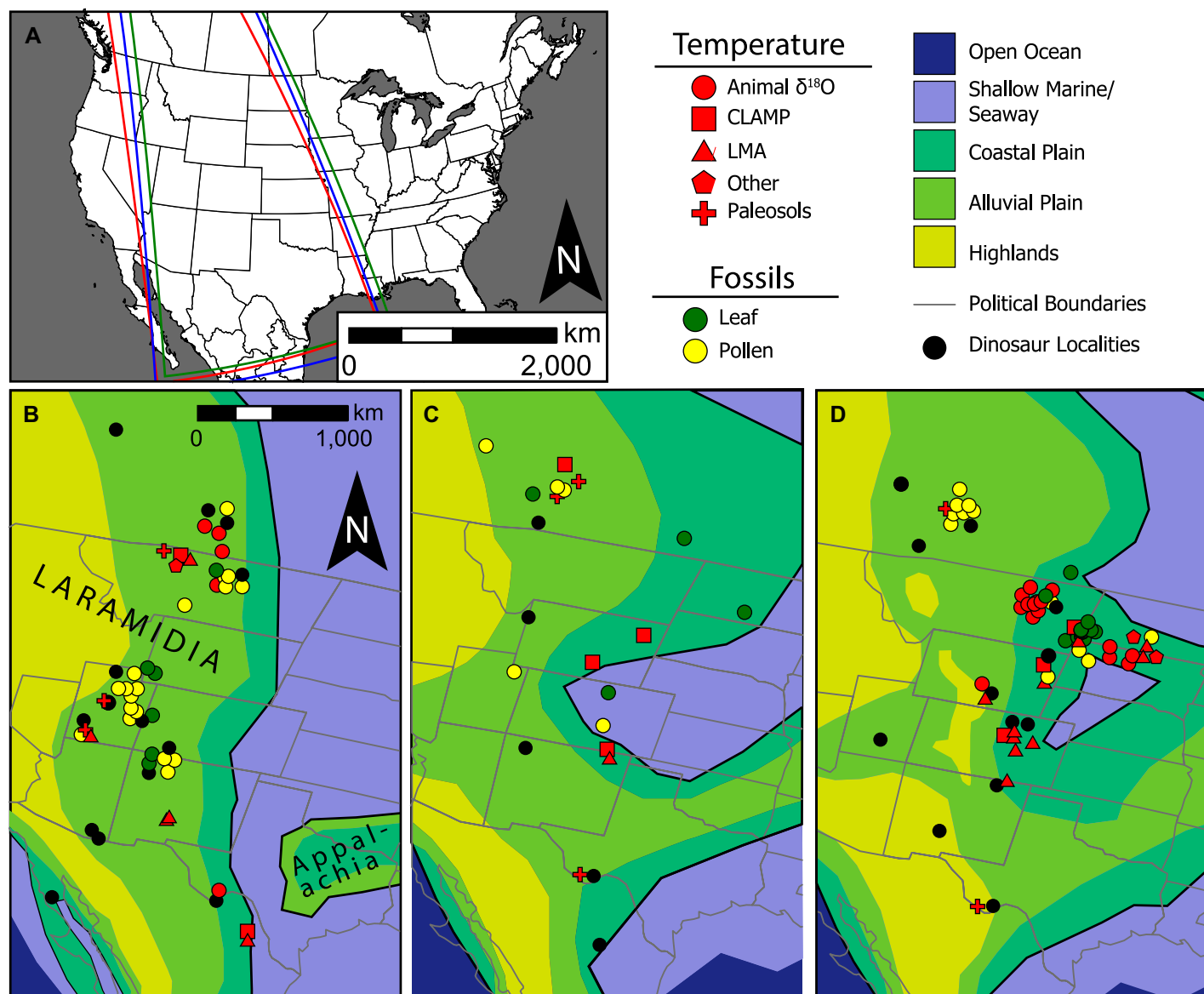


**Figure 1.** Locality map showing the temperature (red symbols), fossil pollen (yellow circles), and fossil leaf (green circles) sites used in this study. (A) Modern study areas. (B) Paleogeographic map of the WIB during the late Campanian (red bounding box in A). (C) WIB during the early Maastrichtian (blue bounding box in A). (D) WIB during the early Maastrichtian (green bounding box in A). The positions of relevant dinosaur fossil localities are marked by black circles. Paleogeography modified from Scotese and Wright (2018) and Blakey (2014). CLAMP—Climate Leaf Analysis Multivariate Program; LMA—Leaf Margin Analysis.

Both the Western Interior Seaway and the cordillera were expressions of global and regional tectonic processes that shaped western North America from the Jurassic to early Cenozoic (Kauffman and Caldwell, 1993). Major Sevier-related thrusting began during the Albian and continued into the early Paleogene, eventually producing high, Andean-style topography along the cordillera (Hildebrand, 2013). Beginning in the early Campanian and continuing into the mid-Cenozoic, the Laramide orogeny produced numerous uplift-bounded intermontane basins that segmented the central United States portion of the Western Interior Basin (Hildebrand, 2013). Gates et al. (2012) suggested that major Laramide tectonism during the Campanian and Maastrichtian was one of the primary drivers of dinosaur diversification during this time.

The Western Interior Seaway was an epeiric sea that first flooded the Western Interior foreland basin in the Early Cretaceous, reached its maximum extent during the Turonian (ca. 94 Ma), and then entered a staggered regression that lasted into the Paleogene (Kauffman and Caldwell, 1993). During the Campanian and the early Maastrichtian, the seaway connected cool Arctic and warm tropical water masses. During the late Maastrichtian, it was separated into isolated northern and southern arms that prevented mixing of the Arctic and tropical waters (Kauffman and Caldwell, 1993).

Circulation in the Western Interior Seaway drove the mixing of cold Arctic and warm tropical waters across an extensive latitudinal boundary zone in the central part of the seaway. Modeling suggests that during periods when the northern and southern portions of the seaway were connected, Arctic and tropical waters were transported south and north via a counterclockwise gyre (Steel et al., 2012). Flögel et al. (2005) divided the central seaway into two zones defined in part by the primary source of ocean water (Arctic or tropical). They recognized a northern ( $>51^{\circ}$  N paleolatitude) zone characterized by relatively low-salinity, brackish Arctic seawater (MAT: 7–10 °C) and a central ( $<51^{\circ}$  N paleolatitude) zone characterized by high-salinity tropical seawater (MAT: 18–28 °C). Other studies (e.g., Coulson et al., 2011) have also reported evidence of a similar oceanic front between cold Arctic and warm tropical waters in both the Turonian and Campanian, although the exact latitudinal location of the boundary varied in each study.

#### Paleoclimate and Paleoenvironmental Conditions of the Western Interior Basin

The Late Cretaceous was a greenhouse period characterized by elevated surface temperatures and reduced latitudinal temperature gradients relative to the modern. Globally averaged MATs

were 6–14 °C warmer than the modern MATs (Niezgodzki et al., 2017). Terrestrial and marine mean latitudinal temperature gradients ranged from 0.3 °C to 0.4 °C °latitude<sup>-1</sup>, compared to modern values of 0.6–1 °C °latitude<sup>-1</sup> (Zhang et al., 2019).

Late Cretaceous Western Interior Basin fossil pollen and leaf assemblages have been reported since the late nineteenth century. Fossil pollen assemblages show that most of North America, including the Western Interior Basin, was part of the *Aquilapollenites* zone, which also included much of eastern Asia (Vajda and Bercovici, 2014). Campanian and Maastrichtian Western Interior Basin climax floras south of  $\sim 46$ –50°N were characterized by tropical to subtropical, sub-humid, open-canopy, broad-leaf evergreen woodlands (Wolfe and Upchurch, 1987). North of 48°N, the vegetation was characterized by a mosaic of temperate sub-humid, broad-leaf evergreen woodlands and forests (Wolfe and Upchurch, 1987).

Despite these general constraints on Late Cretaceous climate and environmental conditions, it is challenging to relate climate to vertebrate paleobiogeography in the Western Interior Basin since most previous quantitative climate and environmental reconstructions are either too broad (e.g., global) or too narrow (e.g., a single site) in focus. The compiled temperature and vegetation data sets and interpolated maps presented in this study provide new constraints on the climate and environment of the Campanian and Maastrichtian Western Interior Basin and shed light on the impact of climate spatial patterns on primary producer distribution across the Western Interior Basin.

#### MATERIALS AND METHODS

Quantitative MAT reconstructions for the Western Interior Basin were collected from the primary literature (Data sets S1 and S2<sup>1</sup>). Isotope-based temperatures ( $\delta^{18}\text{O}$  and clumped isotopes) that were identified by the original authors as diagenetically altered were excluded. Temperature reconstructions without uncertainty estimates (e.g., Van Boskirk, 1998) were assigned conservative estimates based on more recent studies (e.g., leaf margin analysis uncertainties calculated by Peppe et al., 2011). Temperature estimates from the same site were averaged together, resulting in a mean MAT estimate for each unique site in the Campanian and two

Maastrichtian analysis windows. Three analysis windows were chosen with the goal of minimizing the amount of time averaging imposed on our interpolations, while still retaining at least 10 unique localities for the spatial interpolation calculations (Table S1; see footnote 1). Because two of these analysis windows (Campanian and late Maastrichtian) still covered more than 2 m.y., we used the global Cretaceous temperature curves of Friedrich et al. (2012) and O'Brien et al. (2017) to adjust the temperature data to account for secular changes to global MAT.

We created spatially interpolated maps of MAT for each analysis window using the inverse distance weighting (IDW) method (Shepard, 1968) implemented in the custom MATLAB function *gIDW* (Langella, 2020), which estimates a value (e.g., MAT) at an unsampled location based on the distance-weighted average of values at surrounding, sampled points. A spatial resolution of  $1^{\circ} \times 1^{\circ}$  was chosen for the interpolation following the methods of Hengl (2006). To assess the predictive error of our interpolations, we adopted a jackknifing cross-validation technique to calculate the root mean square error (RMSE) associated with the interpolated temperature maps (Fig. S1; see footnote 1). To account for the uncertainties associated with the compiled temperature reconstructions (mean uncertainty =  $\pm 3$  °C, range =  $\pm 1$  to  $\pm 13$  °C), we employed a Monte Carlo approach to randomly sample temperatures from a normally distributed population of MAT estimates calculated for each site. Following this method, 1000 unique spatial interpolations were calculated for each analysis window to compute the full range of possible temperatures and estimate the uncertainty associated with the interpolations (Fig. S2; see footnote 1). The MAT transition zones were defined as any longitudinally contiguous areas within each analysis window where the latitudinal temperature gradients were significantly steeper than the mean Late Cretaceous gradients for  $>70\%$  of the 1000 interpolations. Latitudinal temperature gradients inside and outside the transition zones were calculated using a multivariate linear regression model. For a complete description of how these transition zones were identified and the regression model details, see the Supplementary Materials (see footnote 1).

Ecoregions simplified for paleo-applications were defined based on available information for sample localities (cf. U.S. Department of Agriculture Levels I and II). For undefined assemblages, both pollen and leaf, an ecoregion was identified by attributing fossil taxa to a modern nearest living relative (unattributed or disputed groups assigned conservatively at higher taxonomic levels) and then linking modern distributions (Global Biodiversity Information

<sup>1</sup>Supplemental Material. Additional methods descriptions, figures, tables, and paleotemperature and paleobotany databases. Please visit <https://doi.org/10.1130/GSAB.S.13486902> to access the supplemental material, and contact [editing@geosociety.org](mailto:editing@geosociety.org) with any questions.

Facility, <https://www.gbif.org>, accessed December 2020) to existing low-resolution ecoregion maps (Omernik and Griffith, 2014). For the fossil pollen and leaf similarity analyses, a database of pollen and leaf identifications per formation was transformed into a presence-absence matrix that included both genus-level and species-level binary scorings using the R package *velociraptr* version 1.1.0 (Zaffos, 2019). Pairwise comparisons of biodiversity using the Dice Similarity Index were performed in the R package *fossil* version 0.4.0 (Vavrek, 2011).

To identify latitudes of maximum difference between the putative southern and northern Western Interior Basin regions, standardized pollen and leaf fossil similarity variances were calculated for each integer of latitude from 40°N to 60°N paleolatitude. To test the hypothesis that a climatic barrier caused two distinct biomes of vegetation, we filtered the similarity results data set into three subsets: 72–80 Ma, 69–78 Ma, and 66–75 Ma. For each of the 20 test latitudes we categorized formations whose paleolatitude fell north or south of the hypothesized boundary into respective North or South bins. Each pairwise similarity calculation was labeled as a North-North, North-South, or South-South comparison. Consecutive tests of within and between biome variance were run to identify the latitude that maximizes the difference between in-group variance (i.e., the absolute value of the difference between the northern and southern similarity variance, N-N or S-S) and between-group variance (N-S). Additionally, we defined the boundaries of a vegetation transition zone as the latitudes where the difference between the between-group variance and in-group variance is minimized. More detailed descriptions of methods and results for all calculations and R code can be found in the Supplementary Materials (see footnote 1).

All spatial interpolation and assemblage similarity calculations were performed with paleolatitudes and paleolongitudes calculated using the GPlates software package (<https://www.gplates.org/>, accessed December 2020; Müller et al., 2018). For consistency, paleocoordinates for all Campanian data were calculated for 75 Ma, and the early and late Maastrichtian paleocoordinates were calculated for 70 Ma. The 75 Ma and 70 Ma paleogeographies of Scotese and Wright (2018) were used for all of the Campanian and early/late Maastrichtian figures, respectively.

## RESULTS

### Mean Annual Temperature Spatial Interpolations

The new Campanian and Maastrichtian MAT spatial interpolations presented in this study

reveal large departures from global latitudinal temperature trends within the Western Interior Basin. A total of 73 Campanian MAT reconstructions from 11 unique sites, 50 early Maastrichtian reconstructions from 13 unique sites, and 51 late Maastrichtian MAT reconstructions from 18 unique sites were compiled from 30 individual studies (Data sets S1 and S2). Mean MATs are 18 °C, 16 °C, and 17 °C for the Campanian, early, and late Maastrichtian analysis windows, respectively.

The results of the IDW spatial interpolations for the three analysis windows are shown in Figure 2 and Table 1. The interpolated temperatures are higher in the Campanian and late Maastrichtian than in the early Maastrichtian, which is consistent with global marine temperature trends (Friedrich et al., 2012; O'Brien et al., 2017). The MAT maps are characterized by: (1) a southern zone (~35°N to ~50°N paleolatitude) of relatively high MATs (20–22 °C) and a shallow mean latitudinal temperature gradient, (2) a “temperature transition zone” (~48°N to ~58°N paleolatitude) of intermediate temperatures and a steep mean latitudinal temperature gradient relative to global Late Cretaceous gradients, and (3) a northern zone (>~58°N paleolatitude) of relatively cold mean MATs (11–14 °C) and a return to shallow latitudinal temperature gradients.

We define the MAT transition zone in each analysis window as the longitudinally contiguous area where  $\geq 70\%$  of 1000 unique interpolated MAP iterations yield a local N-S temperature slope that is steeper than the mean global Late Cretaceous latitudinal temperature gradient (Fig. 3). In the Campanian, the latitudinal extent of the transition zone ranged from 3° to 6° latitude, and the zone is characterized by a clear SE–NW trend. In the early Maastrichtian, the extent of the transition zone was 2° to 11° latitude, and the zone displays a shallow NE–SW trend. In the late Maastrichtian, the extent of the transition was 1° to 7° latitude, and the zone displays a roughly E–W trend.

Mean latitudinal temperature gradients inside and outside of the transition zones were calculated for the interpolated temperatures from each analysis (Table 1). The mean MAT slope outside the transition zone is  $-0.4\text{ }^{\circ}\text{C }^{\circ}\text{latitude}^{-1}$  for the Campanian and early Maastrichtian, and  $-0.5\text{ }^{\circ}\text{C }^{\circ}\text{latitude}^{-1}$  for the late Maastrichtian, consistent with estimates of the global Cretaceous latitudinal temperature gradient (Zhang et al., 2019). In contrast, the mean MAT slope inside the transition zone is  $-1.5\text{ }^{\circ}\text{C }^{\circ}\text{latitude}^{-1}$  for the Campanian,  $-1.3\text{ }^{\circ}\text{C }^{\circ}\text{latitude}^{-1}$  for the early Maastrichtian, and  $-1.6\text{ }^{\circ}\text{C }^{\circ}\text{latitude}^{-1}$  for the late Maastrichtian. To test whether the MAT slopes inside the transition zones were significantly different from the MAT slopes outside

the transition zones, we calculated paired t-tests from more than 12,000 MAT slopes calculated inside and outside the transition zones for each analysis window (Fig. 4). For all three analysis windows, the MAT slopes inside the transition zone are significantly different from the slopes outside the transition zone (Table 1).

### Fossil Pollen and Leaf Similarity Index Results

The pollen and leaf flora Dice similarity index values are generally low ( $\leq 0.3$ ) over both short and long geographic distances (Fig. 5A); however, a few of the spatially and temporally closest pollen pairwise comparisons yield similarity values of up to 0.8. The Campanian and early Maastrichtian leaf flora similarity values exhibit a relatively steady decline with increasing distance. In general, the early Campanian and early Maastrichtian leaf floras yield lower similarity values ( $\leq 0.2$ ) than the mid-Campanian leaf floras (0.15–0.3). The late Maastrichtian samples form two groups of close proximity that are nevertheless distinctly different in similarity. The first group yields low similarity values ( $\sim 0.025$ ), while the second group, despite being more temporally distant, yields a higher similarity value (0.2).

The results of our floral climatic boundary test reveal considerable latitudinal variation in pollen flora similarity variance across the three vegetation study areas. In the Campanian, the standardized variance difference is lowest between ~49°N and 53°N paleolatitude, with a minimum at 50°N paleolatitude (Fig. 5B). The negative excursions in the early and late Maastrichtian standardized variance difference are narrower, and the minima are more positive than in the Campanian (~0.4–0.5 versus ~0.2). The fossil leaf data did not provide enough resolution for an equivalent analysis because of small sample sizes.

### Vegetation Ecoregion Results

Fossil pollen and leaf genera were assigned to eight different “ecoregions” following the criteria outlined in the Materials and Methods section and the Supplementary Materials (Data sets S3 and S4; see footnote 1). In all three analysis windows, genera characteristic of the temperate lowland forest and coastal plain ecoregions dominate the raw pollen specimens, whereas the temperate lowland forest and tropical lowland forest ecoregions dominate the raw leaf specimens (Fig. S3; see footnote 1).

The interpolated pollen and leaf data sets yielded divergent results. The pollen ecoregion data are relatively homogeneous, with temperate lowland forest and coastal plain genera

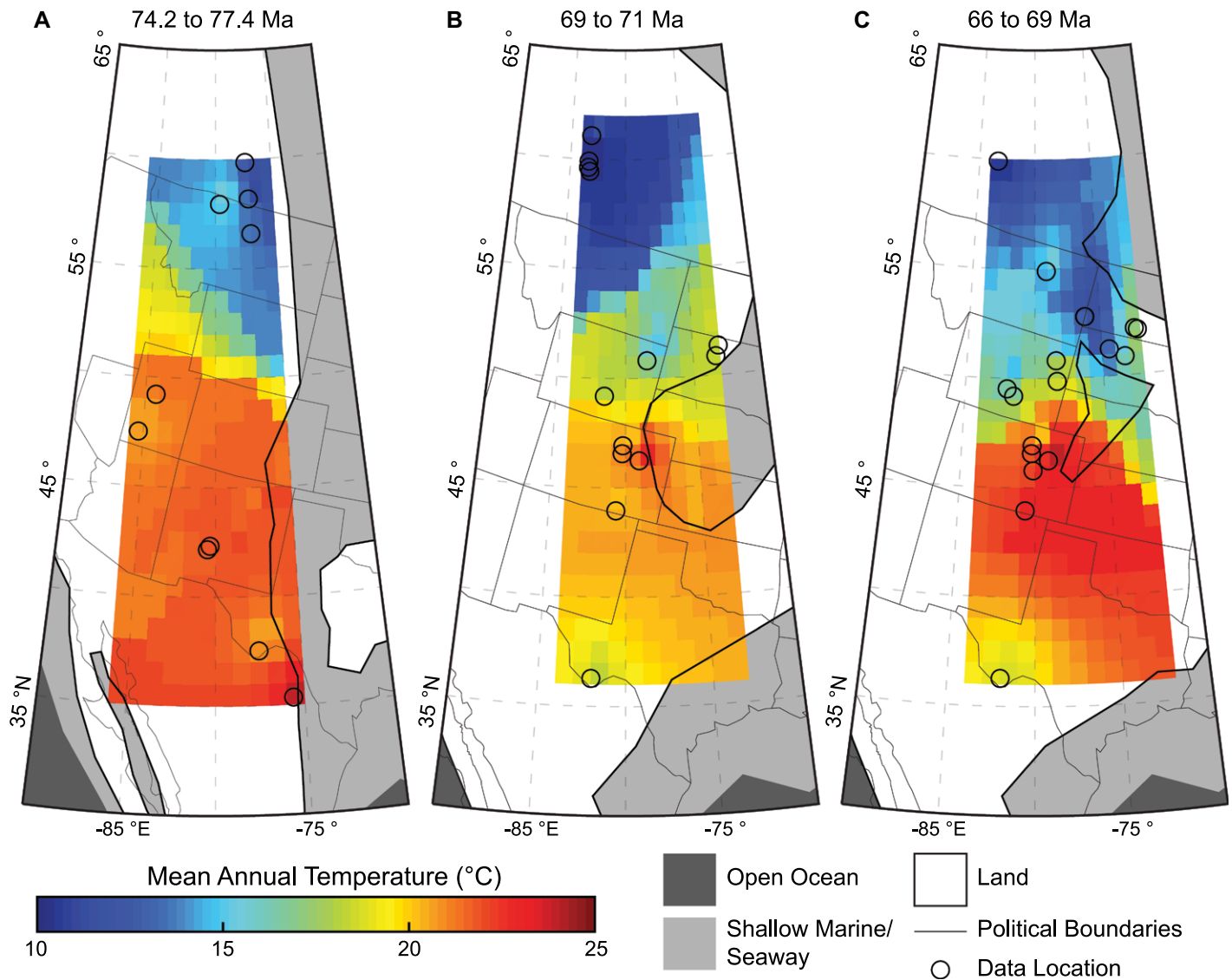


**Figure 2.** Inverse distance weighted spatial interpolation results are shown for (A) the Campanian, (B) early Maastrichtian, and (C) Late Maastrichtian analysis windows.

representing the majority of the identified pollen forms (Fig. S4A–C; see footnote 1). In contrast, the interpolated leaf ecoregion data are more spatially heterogeneous, with the temperate lowland forest ecoregion being the most abundant ecoregion north of  $\sim 55^{\circ}$  paleolatitude and the tropical lowland forest ecoregion being more dominant to the south (Fig. S4D–F).

## DISCUSSION

### A Mean Annual Temperature Transition Zone in the Late Cretaceous Western Interior Basin

The interpolated maps of Late Cretaceous temperature provide clear evidence of a distinct

MAT transition zone with anomalously steep latitudinal temperature gradients. This transition zone divided the central Western Interior Basin into a warmer southern biome that experienced MATs  $>20^{\circ}\text{C}$  and a cooler northern biome with MATs  $<15^{\circ}\text{C}$  (Fig. 2), which is consistent with hypotheses put forward by earlier studies regarding the existence of a climate barrier in the central Western Interior Basin (e.g., Gates et al., 2012).

We hypothesize that these MAT transition zones were produced and maintained by the circulation and spatial climate patterns of the Western Interior Seaway (Fig. 6). During the Campanian, when the northern and southern arms of the seaway were connected, the boundary between 7  $^{\circ}\text{C}$  and 10  $^{\circ}\text{C}$  Arctic waters and 18–28  $^{\circ}\text{C}$  tropi-

cal waters in the central seaway formed a zone of rapidly decreasing sea surface temperatures (SST) from south to north (Hay et al., 1993). We suggest that it was this SST configuration that generated the terrestrial MAT transition zones across the Western Interior Basin alluvial and coastal plains. During the early Campanian, the boundary between these polar and subtropical water masses was located between  $\sim 40^{\circ}\text{N}$  and  $51^{\circ}\text{N}$  paleolatitude (Zhang et al., 2019; Vajda and Bercovici, 2014). In contrast, the mean paleolatitude of the terrestrial late Campanian MAT transition zone identified in this study is  $54^{\circ}\text{N}$  paleolatitude. This may suggest that by the late Campanian, the ocean frontal system in the Western Interior Seaway had migrated northward. The severing of the connection between

TABLE 1. LINEAR REGRESSION MODEL RESULTS DERIVED USING A RANGE OF PLAUSIBLE LATITUDINAL TEMPERATURE THRESHOLDS

Analysis window Age (Ma)	MAT (°C)	RMSE (°C)*	Monte Carlo std. dev. (°C)†	Lat. temp. gradient threshold (°C °lat <sup>-1</sup> )§	Mean SA# slope	Mean TZ** slope	Results on the null hypothesis that mean SA slope minus mean BZ slope = 0				Null hypothesis supported at the 1% significance level?	p-value	t-statistic
							Mean	99% CI Min	99% CI Max				
<u>Campanian</u>													
78–74	18.9	2.3			-0.3 -0.4 -0.5	-0.384 -0.384 -0.384	-1.493 -1.543 -1.587	1.110 1.159 1.203	1.088 1.136 1.179	1.131 1.181 1.226	No No No	0 0 0	133.1 132.5 131.6
78–74 (Adj.)	19.9	2.3	2.4	5.5	-0.4 -0.4 -0.5	-0.420 -0.420 -0.420	-1.637 -1.637 -1.637	1.216 1.216 1.216	1.193 1.239 1.239	1.239 1.281 1.322	No No No	0 0 0	136.3 124.3 124.0
78–74 (Cullen)††	19.0	2.3	2.4	5.9	-0.3 -0.4 -0.5	-0.346 -0.348 -0.349	-1.405 -1.457 -1.505	1.059 1.109 1.156	1.037 1.086 1.132	1.081 1.132 1.180	No No No	0 0 0	123.2
<u>Early Maastrichtian</u>													
71–69	17.3	3.0	2.0	4.9	-0.3 -0.4 -0.5	-0.398 -0.400 -0.402	-1.269 -1.331 -1.377	0.871 0.931 0.975	0.855 0.913 0.957	0.887 0.948 0.994	No No No	0 0 0	141.1 137.8 135.1
71–69 (Adj.)	17.4	3.0	1.9	5.0	-0.4	-0.415	-1.396	0.981	0.963	0.999	No	0	137.4
<u>Late Maastrichtian</u>													
69–66	18.0	3.2	2.3	5.2	-0.3 -0.4 -0.5	-0.448 -0.450 -0.452	-1.598 -1.651 -1.696	1.150 1.201 1.244	1.132 1.182 1.223	1.168 1.220 1.264	No No No	0 0 0	160.9 160.2 158.9
69–66 (Adj.)	18.8	3.2	2.3	5.5	-0.4	-0.446	-1.644	1.198	1.179	1.218	No	0	160.7

Note: BZ—boundary zone.

\*Analytical error calculated using a jackknife resampling approach.

†Mean and maximum standard deviations calculated from 1000 individual standard deviations generated by the Monte Carlo simulation.

§Mean annual temperature (MAT) slopes more negative than the specified threshold value were flagged as potentially being in the transition zone.

#SA—full study area.

\*\*TZ—boundary zone.

††Campanian data with additional data from Cullen et al. (2020).

the northern and southern arms of the seaway by the late Maastrichtian altered its geometry, but the two marine arms still would have permitted Arctic and tropical waters to penetrate into the center of the continent, maintaining the terrestrial MAT transition zones.

The presence of a mid-latitude Western Interior Basin MAT transition zone is consistent with Zhang et al. (2019), who reported similar transition zones in global latitudinal temperature gradients for the Late Cretaceous and Cenozoic. In the marine realm, the position of these temperature gradient “inflection points” is determined by the location of the ocean subtropical and polar fronts, which is in turn determined by the location of the maxima of the westerly winds (Zhang et al., 2019). Modeling of mean annual wind patterns over the Western Interior Seaway suggests that seasonally strong westerlies were responsible for maintaining the ocean frontal system at ~51°N paleolatitude in the Western Interior Seaway (Hay et al., 1993).

Three potential issues with our analysis and interpretation of the Late Cretaceous Western Interior Basin temperature reconstructions are: (1) time-averaging of data from anachronous formations, (2) temperature biases in certain paleotemperature proxies, and (3) the limited number of unique sites for which Late Cretaceous MAT reconstructions are available. To test whether the use of diachronous samples may have produced spurious results in our spatial interpolations, we adjusted the raw MAT estimates to take into account global temperature changes over the Campanian and Maastrichtian, using the global

marine temperature curves of Friedrich et al. (2012) and O’Brien et al. (2017) (see Materials and Methods section for full description). For all three analysis windows, using the adjusted MAT estimates still produces distinct, statistically significant MAT transition zones (Table 1), providing support for our interpretations. Additionally, we note that in both the Campanian and early Maastrichtian analysis windows, the oldest samples are located above 55°N paleolatitude. Longer-term global cooling occurred over the Campanian and early Maastrichtian, which suggests that the older northern samples and younger southern samples in the two data sets are actually warm- and cold-biased, respectively. If this is the case, our spatial reconstructions should be a conservative estimate of the total temperature across the MAT transition zones.

With regard to temperature biases in some paleotemperature proxies, recent work (Cullen et al., 2020) suggested that the single-taxon  $\delta^{18}\text{O}$ -temperature proxies employed by Amiot et al. (2004) suffer from a cold bias and that temperatures in the northern part of our Campanian study area were significantly warmer than previously estimated. However, we suggest that a cold-bias is not likely to have affected our Campanian interpolated MAT results because distinct MAT transition zones are also observed in the early and late Maastrichtian, and the MAT reconstructions from the northern zones of those analysis windows are based on the Climate Leaf Analysis Multivariate Program (CLAMP) and carbonate-clumped isotope paleothermometers rather than the single-taxon  $\delta^{18}\text{O}$  temperature proxy in ques-

tion. Additionally, we note that (1) the incorporation of the warmer Cullen et al. (2020) MAT estimate into our Campanian data set does not significantly alter the resulting interpolated MAT map or our interpretations (Table 1) and (2) after taking into account the uncertainties associated with Amiot et al. (2004) and Cullen et al. (2020) temperature reconstructions, the two estimates are statistically indistinguishable, and the Cullen et al. (2020) reconstructions fall within the range of our interpolated MAT estimates. Finally, while a complete analysis of paleotemperature proxy biases is beyond the scope of this study, we recognize that additional work is needed to resolve the (sometimes major) discrepancies between different paleotemperature proxies.

To test whether the observed MAT transition zones are actually the result of the limited size of our data sets, we performed four additional Monte Carlo simulations for each analysis window. In each simulation, 5, 10, 15, or 20 new MAT data points were added to our existing Campanian, early Maastrichtian, and late Maastrichtian data sets at random locations across the study area. The temperatures were randomly selected from a distribution with minimum and maximum temperatures of 6 °C and 20 °C, respectively. These temperature limits were chosen as plausible estimates of the range in Late Cretaceous MAT values. The resulting temperatures were then increased or decreased by  $-0.4 \text{ }^{\circ}\text{C }^{\circ}\text{latitude}^{-1}$  to maintain a reasonable Late Cretaceous latitudinal temperature gradient. This process was then repeated 250 times for each simulation. The results of this analysis

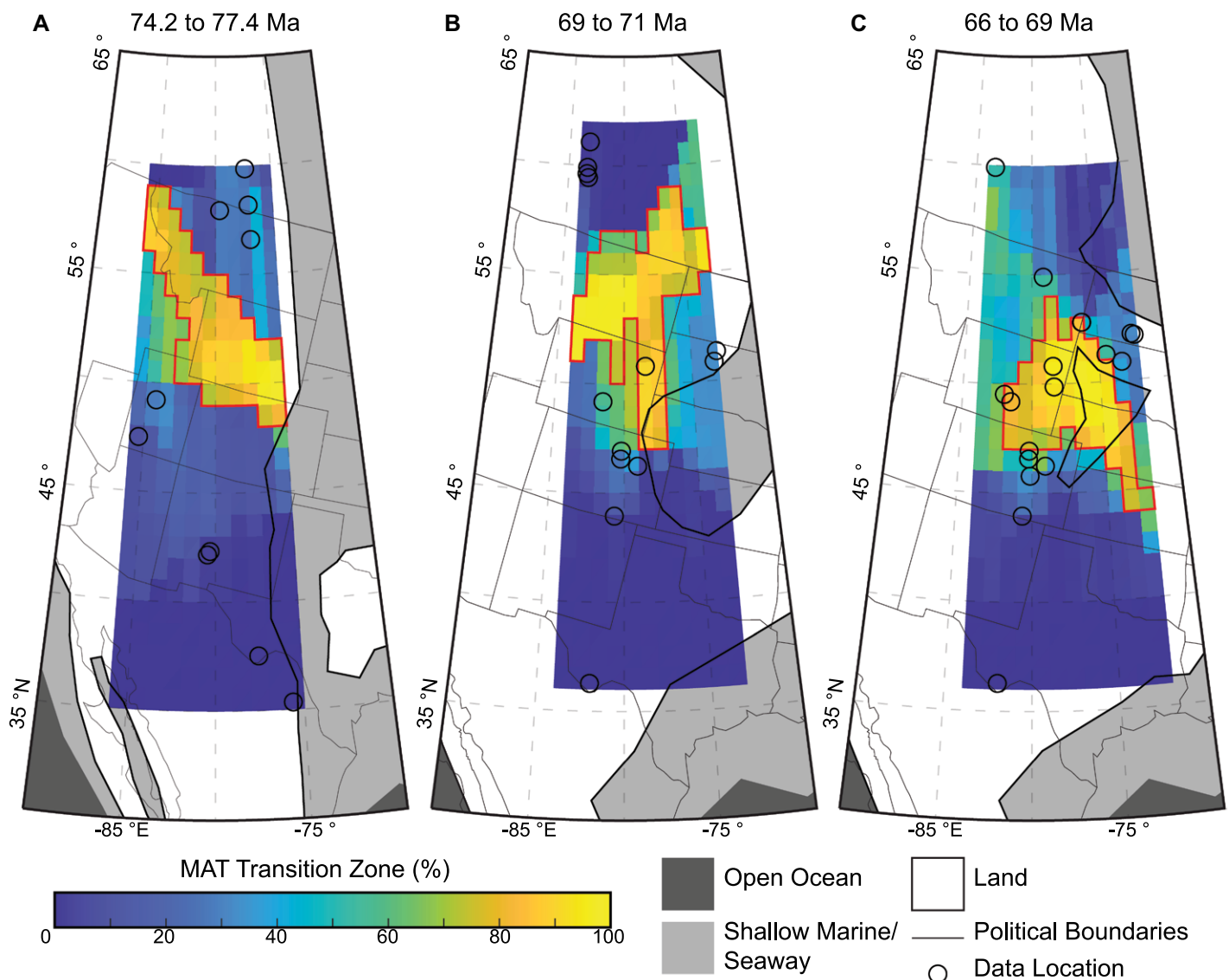


**Figure 3.** Mean annual temperature (MAT) transition zone location is shown for the (A) Campanian, (B) early Maastrichtian, and (C) Late Maastrichtian analysis windows. In each panel, the red line bounds the areas where individual cells were identified as being inside the MAT transition zone in at least 70% of the 1000 Monte Carlo simulations.

show that even when the number of MAT reconstructions in each data set is more than doubled, spatial interpolation still produces strong MAT transition zones with mean latitudinal temperature gradients that are statistically distinct from the full study area gradients (Table S2; see footnote 1).

#### Evidence for Floral Ecological Partitioning in the Late Cretaceous Western Interior Basin

The low, but greater than zero, Dice Similarity Index values ( $\sim 0.2$ ) from our long-distance pairwise pollen flora comparisons suggest that a small, common subset of primary produc-

ers existed across the Western Interior Basin. Additionally, the equally low similarity values for most of the short-distance pollen flora comparisons are consistent with locally unique plant communities. Together, these two observations suggest that during the Late Cretaceous, local floras exhibited higher alpha diversity and lower beta diversity.

The standardized similarity variance results, based on pairwise similarity as a metric for floral regional isolation, demonstrate a regionalization of plant distributions, which we attribute to the presence of the MAT transition zone in the central Western Interior Basin. Not only are the basic biodiversity similarity values low for our plant data sets, the similarity variance

minimum between hypothesized northern and southern regions overlaps with the MAT transition zones ( $\sim 49\text{--}53^\circ\text{N}$  versus  $48\text{--}58^\circ\text{N}$  paleolatitude, respectively), which is consistent with the hypothesis that during the Late Cretaceous, MAT impacted the spatial distribution patterns of primary producers.

The plant similarity variance results give insight into the differing impacts the climatic boundary had during the three time windows. During the Campanian, the negative excursion in the standardized similarity variance data is both deeper and latitudinally wider as compared to during the early and late Maastrichtian (Fig. 5B). This pronounced minimum during the Campanian coincides with the highest Earth-surface temperatures

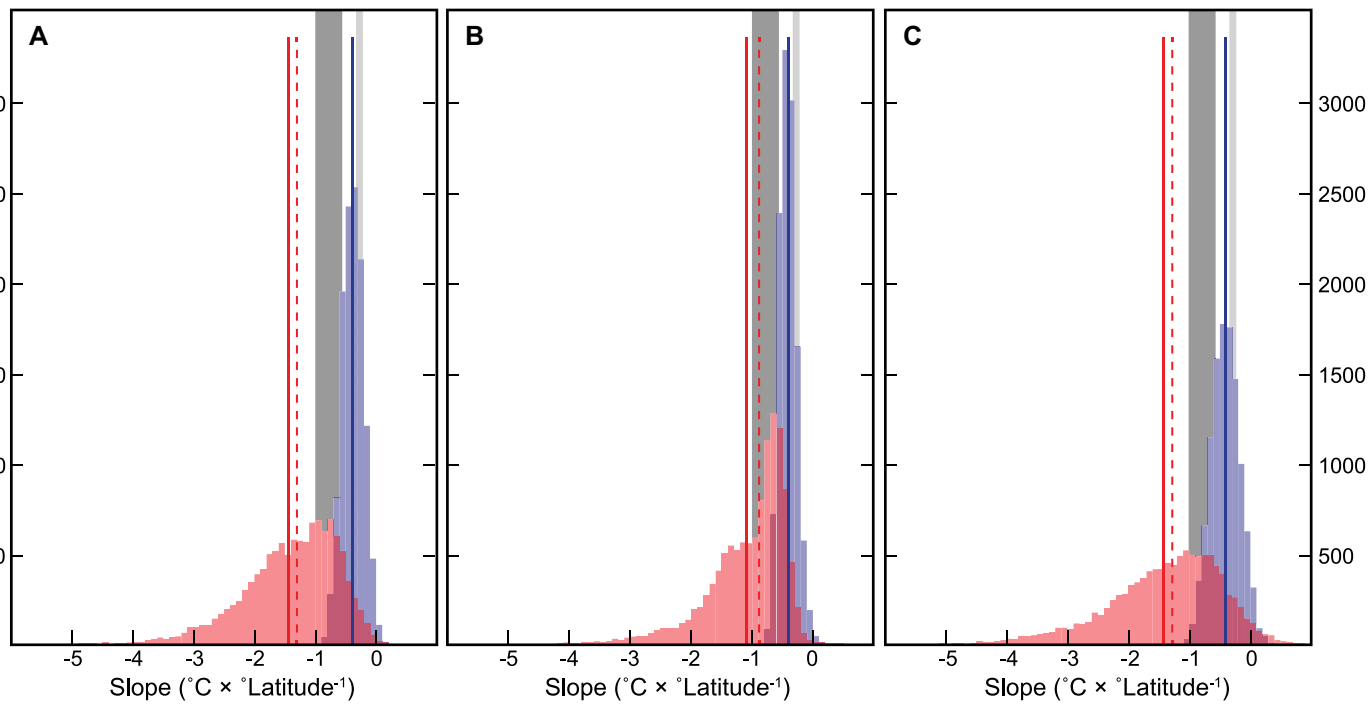


**Figure 4.** Histograms of mean annual temperature (MAT) slopes (latitudinal temperature gradients) inside (red) and outside (blue) the MAT transition zones are shown for (A) the Campanian, (B) early Maastrichtian, and (C) Late Maastrichtian analysis windows. Solid red and blue lines are the mean MAT slopes. Dashed red and blue lines are the median MAT slopes. Dark gray and light gray shaded areas are the mean modern and Late Cretaceous global latitudinal temperature gradients, respectively.

and the maximum extent of the Western Interior Seaway observed in our data sets, suggesting that the combination of high temperatures and reduced land area drove increased primary producer regionalism. In contrast, the shallower, narrower negative standardized similarity variance excursions in the early and late Maastrichtian appear to be due to different mechanisms. During the early Maastrichtian, the lower MATs reduced environmental restrictions on plants expanding southward. In the late Maastrichtian, the retreat of the Western Interior Seaway opened newly habitable land for colonization, potentially counteracting the effect of higher MATs (Weishampel and Horner, 1987; Chiarenza et al., 2019). Alternatively, the smaller negative similarity variance excursions in the Maastrichtian may be due in part to a sampling bias, as our data set contains few records from the southern portion of the Western Interior Basin for these time periods.

Raw and interpolated fossil pollen and leaf data suggest that during the Campanian and Maastrichtian there were distinct environmental (e.g., changes in ecoregion abundance) and compositional (e.g., changes in the dominant plant families and genera within a given ecoregion) differences between the southern and northern biomes. In all three analysis windows, the southern biome is characterized by a patchwork of tropical and temperate lowland forest leaf floras

that likely dominated bank and flood plain depositional environments. However, in the northern biome, the abundance of the tropical lowland forest leaf forms decreases by 14–36%, and the abundance of temperate lowland forest forms increases by 6–20% (Fig. S4D–F). The estuarine or aquatic and wet or successional ecoregions also show large south/north changes in abundance (7% and 10% higher abundance in the northern biome, respectively).

Ecoregion compositional changes are evident in both the fossil pollen and leaf records. Of the 10 most abundant temperate lowland forest leaf genera identified in the Campanian southern biome, only two are also found in the 10 most abundant temperate lowland forest genera in the northern biome. This situation holds true for the early Maastrichtian and late Maastrichtian fossil leaf data as well (Data sets S5A and S5B; see footnote 1). With respect to pollen, of the 10 most abundant early Maastrichtian swampy or lagoonal genera in the south, only two genera are also found in the 10 most abundant genera in the north. Together, the similarity variance and ecoregion abundance/compositional differences between the southern and northern Western Interior Basin provinces suggest that the two regions were environmentally distinct from at least the middle Campanian through the late Maastrichtian and that the spatial patterns

in primary producer distributions were aligned with the regional spatial MAT patterns (Fig. 6).

We note two potential challenges to our interpretation of the fossil pollen and leaf similarity results and ecoregion reconstructions. First, due to the fact that the mean transport distance of pollen is much greater than that of shed leaves, we suggest that our fossil leaf results are representative of local environmental conditions, and the fossil pollen results are generally representative of regional conditions. Second, to have sample populations large enough for analysis, our vegetation analysis windows incorporate much larger time spans than our MAT analysis windows. However, combining data across the wide time windows should dampen smaller signals in the data. Therefore, the observation that a regional change in vegetation exists across the temporal range of our analysis windows likely underestimates its true magnitude, which suggests that the actual difference in vegetation across the floral boundary may have been even more pronounced than is indicated in Figure 6.

#### Impact of Climate and Environmental Transition Zones on the Ecological Regionalization of Vertebrates

Our analyses suggest that the sharp Late Cretaceous MAT transitional zone drove the

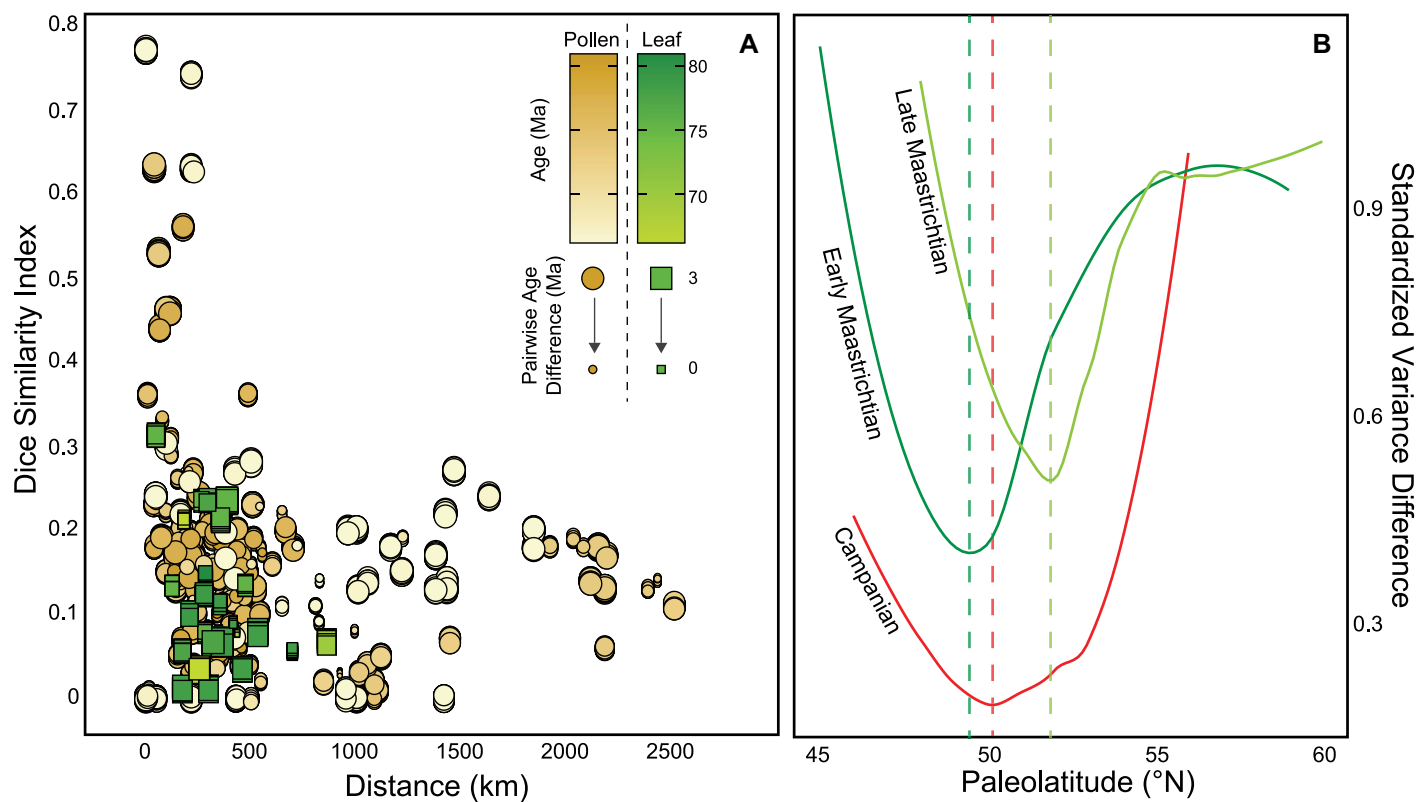


**Figure 5.** Floral biogeographic effects due to climatic barrier are shown. (A) Pollen (yellow circles) and leaf (green squares) similarity plotted against distance between pairwise sites. Marker size (circles and squares) indicates the time difference between pairwise formations. The maximum time gap between formations is 3 m.y., and the minimum is ca. 0 m.y. (B) LOESS (locally weighted smoothing) plot of difference between in-group similarity variance difference and the out-group similarity variance, standardized to 1, plotted against latitude. Lowest points in each line represent the approximate latitudinal position of maximum change in flora between the northern and southern biomes (vertical dashed lines).

regionalization of distinct southern and northern biomes of primary producers and that these biomes varied in the abundance and composition of floral assemblages. Such differences would be expected to translate across trophic networks, exerting some control on the distribution and evolution of vertebrate clades—particularly herbivores—throughout the Western Interior Basin during the terminal Cretaceous (Owen-Smith, 1992). However, any potential cascading effects of primary producer regionalization on ecological networks within the Western Interior Basin during the Late Cretaceous are currently unknown.

The most taxonomically comprehensive attempt at parsing out vertebrate distribution patterns across the Western Interior Basin in the Late Cretaceous was conducted by Gates et al. (2010), who analyzed the distribution of fish, squamates, lissamphibians, dinosaurs, and mammals across the Western Interior Basin during the Campanian. Using vertebrate presence/absence and relative abundance data they demonstrated that northern and southern communi-

ties were highly divergent in terms of species composition, but they could not discriminate the nature of the “boundary” and found the scenarios of northern and southern biomes with an intermediate zone of faunal mixing and a continuous latitudinal faunal gradient to be equally likely. Gates et al. (2010) also noted that patterns of distribution varied by taxonomic group, implying clade-specific relationships between MAT and Western Interior Basin vertebrates. For example, the observed regionalization of some fish taxa was speculated to be related to their high reliance on surface water temperature (Gates et al., 2010). Regionalization was also noted for some amphibians, turtles, and squamates. In contrast, mammals and dinosaur species were found to be largely restricted to individual formations and therefore failed to support any scenario when considered historically.

Several papers have suggested that the lack of taxonomically informative skeletal material of dinosaurs from across a large latitudinal swath of Upper Cretaceous formations in the Western Interior Basin at <300 k.y. intervals falsifies a

hypothesis of latitudinally restricted biomes in the Western Interior Basin (Fowler, 2006; Sullivan and Lucas, 2006; Fowler, 2017; Chiarenza et al., 2019). However, given that nearly all dinosaur species distributions are restricted to a single Western Interior Basin formation, the lack of contemporaneous species data cannot falsify a hypothesis of multiple restricted biozones, just as it cannot falsify an alternative hypothesis of continent-scale uniform ranges in Late Cretaceous dinosaurs. The question of regionalization is perhaps more confidently approached through a phylogenetic lens, which circumvents issues of diachroneity in species data and subjectivity in taxonomic assignment. Most recent studies arguing for regionalization suggest that it manifests via evolutionary centers (albeit sometimes “leaky” centers) and is traceable through temporally calibrated phylogenies coupled with biogeographic data (Sampson et al., 2010, 2013; Loewen et al., 2013; Lund et al., 2016; Ryan et al., 2017; Fowler and Freedman Fowler, 2020).

The presence of ecoregions associated with changes in primary producer composition and

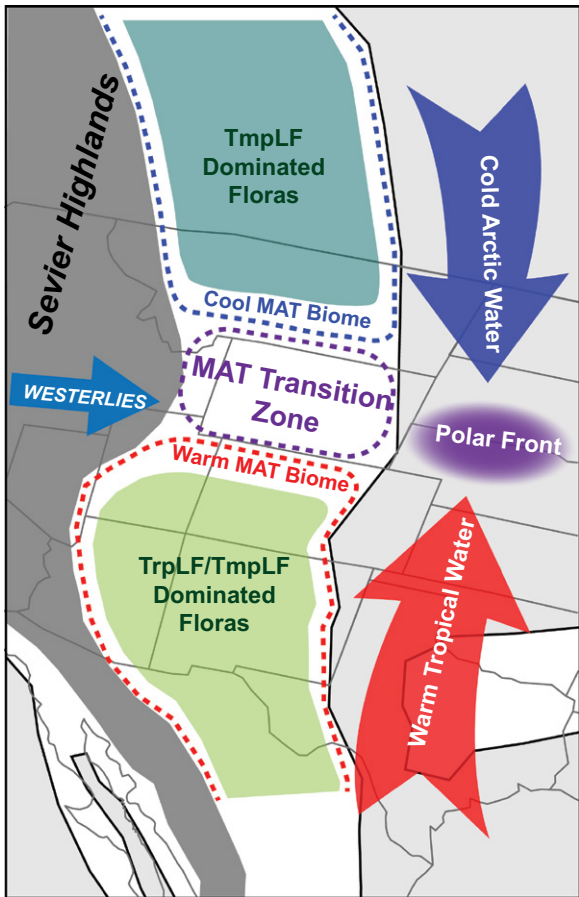


**Figure 6.** Schematic map of the Campanian Western Interior Basin illustrates the climatic and floral zones and the paleoceanographic conditions hypothesized to give rise to the terrestrial mean annual temperature (MAT) transition zone. TmpLF—temperate lowland forest; TrpLF—tropical lowland forest.

clades (e.g., Sampson et al., 2010, 2013; Loewen et al., 2013; Lund et al., 2016; Ryan et al., 2017; Fowler and Freedman Fowler, 2020; but see Longrich [2014] for an alternative viewpoint).

Ultimately, our data demonstrate that an abrupt climate transition bounded by distinct biomes characterized the Western Interior Basin throughout most of the terminal Cretaceous. This recognition sets the stage for further hypothesis testing around geographic centers of dinosaur evolution in the region and different dietary habits among megaherbivorous clades (e.g., hadrosaurs and ceratopsians) and/or subclades (centrosaur subclades) that could translate to differential susceptibility to variation in primary producer composition and abundance across the Western Interior Basin.

## CONCLUSIONS

This study provides the first clear evidence for climatic and environmental controls on biogeography of primary producers in the Late Cretaceous Western Interior Basin. Our spatial MAT interpolations support the hypothesis that a distinct climate barrier existed in the central Western Interior Basin in the form of a temperature transition zone characterized by exceptionally steep latitudinal temperature gradients. Additionally, our fossil vegetation ecoregion and flora similarity analyses show that the Late Cretaceous Western Interior Basin was characterized by distinct southern and northern vegetation biomes. The boundary between these two zones coincides with the reconstructed MAT transition zone, which we interpret as evidence that spatial climate patterns across the Western Interior Basin impacted vegetation distribution over a broad region. Finally, our reconstructions show that both the temperature and vegetation transition zones evolved over the course of the Campanian and Maastrichtian, likely in response to global climate change and the shifting geography of the Western Interior Seaway.

Currently, constraints on seasonal temperatures (e.g., coldest and warmest mean monthly temperatures) across the Western Interior Basin are lacking. Future studies should aim to address this gap in our knowledge, since seasonal temperature extremes act as important controls on primary producer distributions (e.g., Huber, 2008).

Although the Late Cretaceous vertebrate fossil record of the Western Interior Basin remains temporally too sparse to confirm whether or not vertebrate groups such as dinosaurs also exhibited climate- and environment-induced endemicity, the findings presented in this study provide important evidence that Late Cretaceous climate patterns shaped the evolution of vegetation

MAT documented here provides a potential underlying cause for different distributions of dinosaur taxa within the Western Interior Basin. Using modern North American climate gradients and ecosystems as a proxy for the Cretaceous, the climatic boundary deciphered in this study transitioned from a MAT of 11 °C to a MAT of 18 °C over a mean distance of ~3.3° latitude. Within the southeastern United States today, the same temperature transition occurs over 7.3° latitude (e.g., between Richmond, Virginia, and Tallahassee, Florida)—more than twice the distance. Such a strong climatic barrier and associated fundamental forest restructuring over a short geographic distance may have been sufficient to produce latitudinally distinct centers of evolution and, over extended periods of geologic time, produce regionalized biomes. However, to date, almost all studies assessing the potential co-evolution of dinosaurs and plants are too coarse in scope and scale to inform regional macroevolutionary patterns in Western Interior Basin herbivorous dinosaur assemblages (e.g., Weishampel and Norman, 1989; Tiffney, 1992; Coe et al., 1987; Barrett and Willis, 2001; Butler et al., 2009a, 2009b, 2010), and the vast majority of proposed diets for individual mega-

herbivorous taxa based on direct evidence of diet are either questionable associations or uninformative at lower taxonomic levels (Mallon and Anderson, 2013). Moreover, although plant-dinosaur associations have been proposed to drive macroevolutionary and biogeographic trends among major dinosaur clades, it is as of yet unclear if such trends would manifest at the subclade level, which is the resolution on which most modern arguments of distinct dinosaur biomes in the Western Interior Basin are based. As a case in point, although Mallon and Anderson (2013) presented evidence against the idea that niche partitioning is observed at the genus or species level in major clades of Western Interior Basin megaherbivores, their study only tests the effect of niche partitioning on taxa within a single geological formation, the Dinosaur Park Formation, and cannot be extrapolated widely across different megaherbivore communities in the Western Interior Basin. Whereas Ryan et al. (2017) note that the divergent ecomorphology of some more recently recognized centrosaurine subclades (e.g., nasutoceratopsians) may have resulted in niche partitioning in lower taxonomic groups. Such a pattern fits with recognition of potential regionalization of ceratopsian sub-

communities in western North America for the final 12 m.y. of the Mesozoic Era.

## ACKNOWLEDGMENTS

This work was funded by National Science Foundation Award 1925973 (E. Hyland and L.E. Zanno). Additionally, the authors thank the Paleo<sup>3</sup> Research Group at North Carolina State University for their comments and suggestions and Christopher Scotese for technical assistance with GPlates and Point Tracker software.

## REFERENCES CITED

Alroy, J., 2010, Geographical, environmental and intrinsic biotic controls on Phanerozoic marine diversification: *Palaeontology*, v. 53, no. 6, p. 1211–1235, <https://doi.org/10.1111/j.1475-4983.2010.01011.x>.

Amiot, R., Lécyer, C., Buffetaut, E., Fluteau, F., Legendre, S., and Martineau, F., 2004, Latitudinal temperature gradient during the Cretaceous Upper Campanian–Middle Maastrichtian:  $^{87}\text{Sr}$  record of continental vertebrates: *Earth and Planetary Science Letters*, v. 226, no. 1–2, p. 255–272, <https://doi.org/10.1016/j.epsl.2004.07.015>.

Anderson, P.S.L., Friedman, M., Brazeau, M.D., and Rayfield, E.J., 2011, Initial radiation of jaws demonstrated stability despite faunal and environmental change: *Nature*, v. 476, p. 206–209, <https://doi.org/10.1038/nature10207>.

Arbour, V.M., Zanno, L.E., and Gates, T., 2016, Ankylosaurian dinosaur palaeoenvironmental associations were influenced by extirpation, sea-level fluctuation, and geodispersal: *Palaeo*, v. 449, p. 289–299, <https://doi.org/10.1016/j.palaeo.2016.02.033>.

Barrett, P.M., 2014, Paleobiology of herbivorous dinosaurs: *Annual Review of Earth and Planetary Sciences*, v. 42, p. 207–230, <https://doi.org/10.1146/annurev-earth-042711-105515>.

Barrett, P.M., and Willis, K.J., 2001, Did dinosaurs invent flowers? Dinosaur–angiosperm coevolution revisited: *Biological Reviews of the Cambridge Philosophical Society*, v. 76, p. 411–447, <https://doi.org/10.1017/S1464793101005735>.

Berry, K., 2018, Paleontological evidence against a major geographic barrier at about the paleolatitude of Colorado, USA, during the Late Campanian (Late Cretaceous): The conspicuous absence of endemic subclades of chasmosaurine ceratopsid (horned) dinosaurs and its significance: *The Mountain Geologist*, v. 55, no. 1, p. 5–18, <https://doi.org/10.31582/rmag.mg.55.1.5>.

Blakely, R.C., 2014, Paleogeography and paleotectonics of the Western Interior Seaway, Jurassic–Cretaceous of North America: *Search and Discovery*, v. 30392, 77 p.

Butler, R.J., Barrett, P.M., Kenrick, P., and Penn, M.G., 2009a, Diversity patterns amongst herbivorous dinosaurs and plants during the Cretaceous: Implications for hypotheses of dinosaur/angiosperm co-evolution: *Journal of Evolutionary Biology*, v. 22, no. 3, p. 446–459, <https://doi.org/10.1111/j.1420-9101.2008.01680.x>.

Butler, R.J., Barrett, P.M., Kenrick, P., and Penn, M.G., 2009b, Testing co-evolutionary hypotheses over geological timescales: Interactions between Mesozoic non-avian dinosaurs and cycads: *Biological Reviews of the Cambridge Philosophical Society*, v. 84, p. 73–89, <https://doi.org/10.1111/j.1469-185X.2008.00065.x>.

Butler, R.J., Barrett, P.M., Fls, P.K., and Penn, M.G., 2010, Testing coevolutionary hypotheses over geological timescales: Interactions between Cretaceous dinosaurs and plants: *Biological Journal of the Linnean Society*, v. 100, no. 1, p. 1–15, <https://doi.org/10.1111/j.1095-8312.2010.01401.x>.

Chiarenza, A.A., Mannion, P.D., Lunt, D.J., Farnsworth, A., Jones, L.A., Kelland, S., and Allison, P.A., 2019, Ecological niche modelling does not support climatically-driven dinosaur diversity decline before the Cretaceous/Paleogene mass extinction: *Nature Communications*, v. 10, no. 1, p. 1–14, <https://doi.org/10.1038/s41467-019-08997-2>.

Coe, M., Dilcher, D., Farlow, J., Jarzen, D., and Russell, D., 1987, Dinosaurs and land plants, in Friis, E., Chaloner, W., and Crane, P., eds., *Origins of Angiosperms and Their Biological Consequences*: New York, Cambridge University Press, 372 p.

Coulson, A.B., Kohn, M.J., and Barrick, R.E., 2011, Isotopic evaluation of ocean circulation in the Late Cretaceous North American seaway: *Nature Geoscience*, v. 4, no. 12, p. 852–855, <https://doi.org/10.1038/ngeo1312>.

Cullen, T.M., Longstaffe, F.J., Wortmann, U.G., Huang, L., Fanti, G.S.T.F., Goodwin, M.B., and Evans, D.C., 2020, Large-scale stable isotope characterization of a Late Cretaceous dinosaur-dominated ecosystem: *Geology*, v. 48, no. 6, p. 546–551, <https://doi.org/10.1130/G47399.1>.

Dean, C.D., Chiarenza, A.A., and Maidment, S.C.R., 2020, Formation binning: A new method for increased temporal resolution in regional studies, applied to the Late Cretaceous dinosaur fossil record of North America: *Palaeontology*, v. 63, p. 881–901, <https://doi.org/10.1111/pana.12492>.

Flögel, S., Hay, W.W., DeConto, R.M., and Balukhovsky, A.N., 2005, Formation of sedimentary bedding couplets in the Western Interior Seaway of North America — Implications from climate system modeling: *Palaeogeography, Palaeoclimatology, Palaeoecology*, v. 218, p. 125–143, <https://doi.org/10.1016/j.palaeo.2004.12.011>.

Fowler, D., 2006, Terrestrial Late Cretaceous stratigraphy of North America and the utility of ceratopsids in biostratigraphy: *Journal of Vertebrate Paleontology*, v. 26, p. 63A.

Fowler, D.W., 2017, Dinosaur stratigraphic ranges of the Santonian–Maastrichtian (Late Cretaceous) formations of the Western Interior of North America: *PLoS ONE*, v. 12, no. 11, no. e0188426, p. 1–20, <https://doi.org/10.1371/journal.pone.0188426>.

Fowler, D.W., and Freedman Fowler, E.A., 2020, Transitional evolutionary forms in chasmosaurine ceratopsid dinosaurs: Evidence from the Campanian of New Mexico: *Peer J: Life and Environment*, v. 8, no. e9251, <https://doi.org/10.7717/peerj.9251>.

Friedrich, O., Norris, R.D., and Erbacher, J., 2012, Evolution of middle to Late Cretaceous oceans—A 55 m.y. record of Earth's temperature and carbon cycle: *Geology*, v. 40, no. 2, p. 107–110, <https://doi.org/10.1130/G32701.1>.

Gates, T.A., Sampson, S.D., Zanno, L.E., Roberts, E.M., Eaton, J.G., Nydam, R.L., Hutchison, J.H., Smith, J.A., Loewen, M.A., and Getty, M.A., 2010, Biogeography of terrestrial and freshwater vertebrates from the late Cretaceous (Campanian) Western Interior of North America: *Palaeogeography, Palaeoclimatology, Palaeoecology*, v. 291, p. 371–387, <https://doi.org/10.1016/j.palaeo.2010.03.008>.

Gates, T.A., Prieto-Márquez, A., and Zanno, L.E., 2012, Mountain building triggered Late Cretaceous North American megaherbivore dinosaur radiation: *PLoS ONE*, v. 7, no. 8, p. 1–10, no. e42135, <https://doi.org/10.1371/journal.pone.0042135>.

Hay, W.W., Eicher, D., and Diner, R., 1993, Physical oceanography and water masses of the Cretaceous Western Interior Seaway, in Caldwell, W.G.E., and Kauffman, E.G., eds., *Evolution of the Western Interior Basin: Geological Association of Canada Special Paper* 39, p. 297–318.

Hengl, T., 2006, Finding the right pixel size: Computers and Geosciences, v. 32, p. 1283–1298, <https://doi.org/10.1016/j.cageo.2005.11.008>.

Hildebrand, R.S., 2013, Mesozoic Assembly of the North American Cordillera: *Geological Society of America Special Paper* 495, 162 p.

Huber, M., 2008, Climate change. A hotter greenhouse?: *Science*, v. 321, p. 353–354, <https://doi.org/10.1126/science.1161170>.

Jablonski, D., 2007, Scale and hierarchy in macroevolution: *Palaeontology*, v. 50, p. 87–109, <https://doi.org/10.1111/j.1475-4983.2006.00615.x>.

Jansson, R., 2003, Global patterns in endemism explained by past climatic change: *Proceedings of the Royal Society B: Biological Sciences*, v. 270, p. 583–590, <https://doi.org/10.1098/rspb.2002.2283>.

Kauffman, E.G., and Caldwell, W.G.E., 1993, The Western Interior Basin in space and time, in Kauffman, E.G., and Caldwell, W.G.E., eds., *Evolution of the Western Interior Basin: Geological Association of Canada Special Publication* 39, no. 2, p. 1–30.

Lamoreux, J.F., Morrison, J.C., Ricketts, T.H., Olson, D.M., Dinerstein, E., McKnight, M.W., and Shugart, H.H., 2006, Global tests of biodiversity concordance and the importance of endemism: *Nature*, v. 440, p. 212–214, <https://doi.org/10.1038/nature04291>.

Langella, G., 2020, Inverse Distance Weighted (IDW) or Simple Moving Average (SMA) interpolation: *MATLAB Central File Exchange*, <https://www.mathworks.com/matlabcentral/fileexchange/27562-inverse-distance-weighted-idw-or-simple-moving-average-sma-interpolation>.

Lehman, T.M., 1987, Late Maastrichtian paleoenvironments and dinosaur biogeography in the western interior of North America: *Palaeogeography, Palaeoclimatology, Palaeoecology*, v. 60, no. C, p. 189–217, [https://doi.org/10.1016/0031-0182\(87\)90032-0](https://doi.org/10.1016/0031-0182(87)90032-0).

Lehman, T.M., 1997, Late Campanian dinosaur biogeography in the western interior of North America, in Wolberg, D.L., Stump, E., and Rosenberg, G.D., eds., *Dinofest International: Proceedings of a Symposium Sponsored by Arizona State University*: Philadelphia, Academy of Natural Sciences, p. 223–240.

Lehman, T.M., 2001, Late Cretaceous dinosaur provinciality, in Tanke, D.H., Carpenter, D.H.K., and Skrepnick, M.W., eds., *Mesozoic Vertebrate Life*: Bloomington, Indiana, Indiana University Press, p. 310–328.

Lehman, T.M., McDowell, F.W., and Connelly, J.N., 2006, First isotopic (U–Pb) age for the Late Cretaceous Alamosaurus vertebrate fauna of west Texas, and its significance as a link between two faunal provinces: *Journal of Vertebrate Paleontology*, v. 26, no. 4, p. 922–928, [https://doi.org/10.1671/0272-4634\(2006\)26\[922:FIAT\]2.0.CO;2](https://doi.org/10.1671/0272-4634(2006)26[922:FIAT]2.0.CO;2).

Leslie, C.E., Peppe, D.J., Williamson, T.E., Heizler, M., Jackson, M., Atchley, S.C., Nordt, L., and Standhardt, B., 2018, Revised age constraints for Late Cretaceous to early Paleocene terrestrial strata from the Dawson Creek section, Big Bend National Park, west Texas: *Bulletin of the Geological Society of America*, v. 130, no. 7–8, p. 1143–1163, <https://doi.org/10.1130/B31785.1>.

Lieberman, B.S., 2005, Earth history change: The pace-maker of evolution: *The Paleontological Society Papers*, v. 11, p. 5–14, <https://doi.org/10.1017/S10893260001212>.

Loewen, M.A., Irmis, R.B., Sertich, J.J.W., Currie, P.J., and Sampson, S.D., 2013, Tyrant dinosaur evolution tracks the rise and fall of late Cretaceous oceans: *PLoS ONE*, v. 8, no. 11, <https://doi.org/10.1371/journal.pone.0079420>.

Longrich, N.R., 2014, The horned dinosaurs Pentaceratops and Kosmoceratops from the Upper Campanian of Alberta and implications for dinosaur biogeography: *Cretaceous Research*, v. 51, p. 292–308, <https://doi.org/10.1016/j.cretres.2014.06.011>.

Lucas, S.G., Sullivan, R.M., and Hunt, A.P., 2006, Re-evaluation of Pentaceratops and Chasmosaurus (Ornithischia: Ceratopsidae) in the Upper Cretaceous of the Western Interior: *New Mexico Museum of Natural History and Science Bulletin*, v. 35, p. 367–370.

Lucas, S.G., Sullivan, R.M., Lichtig, A.J., Dalman, S.G., and Jasinski, S.E., 2016, Late Cretaceous dinosaur biogeography and endemism in the Western Interior basin, North America: A critical re-evaluation: *New Mexico Museum of Natural History and Science Bulletin*, v. 71, p. 195–213.

Lund, E.K., O'Connor, P.M., Loewen, M.A., and Jinnah, Z.A., 2016, A New Centrosaurine Ceratopsid, *Machairiceratops cronusi* gen et sp. nov., from the Upper Sand Member of the Wahweap Formation (Middle Campanian), Southern Utah: *PLoS ONE*, v. 11, no. 5, p. 1–21, <https://doi.org/10.1371/journal.pone.0154403>.

Mallon, J.C., and Anderson, J.S., 2013, Skull ecomorphology of megaherbivorous dinosaurs from the Dinosaur Park Formation (Upper Campanian) of Alberta, Canada: *PLoS ONE*, v. 8, no. 7, p. 1–17, <https://doi.org/10.1371/journal.pone.0067182>.

Mayr, E., 1982, Speciation and macroevolution: Evolution; *International Journal of Organic Evolution*, v. 36, no. 6, p. 1119–1132, <https://doi.org/10.1111/j.1558-5646.1982.tb05483.x>.

Müller, R.D., Cannon, J., Qin, X., Watson, R.J., and Gurnis, M., 2018, GPlates: Building a virtual Earth through deep time: *Geochemistry, Geophysics, Geosystems*, v. 19, no. 7, p. 2243–2261, <https://doi.org/10.1029/2018GC007584>.

Niezgodzki, I., Knorr, G., Lohmann, G., Tyszka, J., and Markwick, P.J., 2017, Late Cretaceous climate simulations with different CO<sub>2</sub> levels and subarctic gateway configurations: A model-data comparison: *Paleoceanography*, v. 32, no. 9, p. 980–998, <https://doi.org/10.1002/2016PA003055>.

Nydam, R.L., Rowe, T.B., and Cifelli, R.L., 2013, Lizards and snakes of the Terlingua Local Fauna (late Campanian), Aguja Formation, Texas, with comments on the distribution of paracontemporaneous squamates throughout the Western Interior of North America: *Journal of Vertebrate Paleontology*, v. 33, no. 5, p. 1081–1099, <https://doi.org/10.1080/02724634.2013.760467>.

O'Brien, C.L., Robinson, S.A., Pancost, R.D., Sinningshe Damste, J.S., Schouten, S., Lunt, D.J., Alsenz, H., Bornemann, A., Bottini, C., Brassell, S.C., Farnsworth, A., Forster, A., Huber, B.T., Inglis, G.N., Jenkyns, H.C., Linnert, C., Littler, K., Markwick, P., Mcanena, A., Mutterlose, J., Naafs, B.D.A., Püttmann, W., Sluijs, A., Van Helmond, N.A.G.M., Vellekoop, J., Wagner, T., and Wrobel, N.E., 2017, Cretaceous sea-surface temperature evolution: Constraints from TEX 86 and planktonic foraminiferal oxygen isotopes: *Earth-Science Reviews*, v. 172, p. 224–247, <https://doi.org/10.1016/j.earscirev.2017.07.012>.

Omernik, J.M., and Griffith, G.E., 2014, Ecoregions of the conterminous United States: Evolution of a hierarchical spatial framework: *Environmental Management*, v. 54, p. 1249–1266, <https://doi.org/10.1007/s00267-014-0364-1>.

Owen-Smith, N., 1992, Grazers and browsers: Ecological and social contrasts among African ruminants: Proceedings of the International Symposium Ongulés/Ungulates 91 Toulouse, France, p. 175–181.

Pardo, J.D., Small, B.J., Milner, A.R., and Huttenlocker, A.K., 2019, Constrained early land vertebrate radiations: *Nature Ecology and Evolution*, v. 3, p. 200–206, <https://doi.org/10.1038/s41559-018-0776-z>.

Pepe, D.J., Royer, D.L., Cariglino, B., Oliver, S.Y., Newmann, S., Leight, E., Enikolopov, G., Fernandez-Burgos, M., Herrera, F., Adams, J.M., Correa, E., Curran, E.D., Erickson, J.M., Hinojosa, L.F., Hoganson, J.W., Iglesias, A., Jaramillo, C.A., Johnson, K.R., Jordan, G.J., Kraft, N.J.B., Lovelock, E.C., Lusk, C.H., Niinemets, U., Penuelas, J., Rapson, G., Wing, S.L., and Wright, L.J., 2011, Sensitivity of leaf size and shape to climate: Global patterns and paleoclimatic applications: *The New Phytologist*, v. 190, no. 3, p. 724–739, <https://doi.org/10.1111/j.1469-8137.2010.03615.x>.

Ryan, M.J., Holmes, R., Mallon, J., Loewen, M., and Evans, D.C., 2017, A basal ceratopsid (Centrosaurinae: Nasutoceratopsini) from the Oldman Formation (Campanian) of Alberta, Canada: *Canadian Journal of Earth Sciences*, v. 54, p. 1–14, <https://doi.org/10.1139/cjes-2016-0110>.

Sampson, S.D., and Loewen, M.A., 2005, Tyrannosaurus rex from the Upper Cretaceous (Maastrichtian) North Horn Formation of Utah: Biogeographic and paleoecologic implications: *Journal of Vertebrate Paleontology*, v. 25, no. 2, p. 469–472, [https://doi.org/10.1671/0272-4634\(2005\)025\[0469:TRFTUC\]2.0.CO;2](https://doi.org/10.1671/0272-4634(2005)025[0469:TRFTUC]2.0.CO;2).

Sampson, S.D., Loewen, M.A., Farke, A.A., Roberts, E.M., Forster, C.A., Smith, J.A., and Titus, A.L., 2010, New horned dinosaurs from Utah provide evidence for intracontinental dinosaur endemism: *PLoS ONE*, v. 5, no. 9, p. 1–12, <https://doi.org/10.1371/journal.pone.0012292>.

Sampson, S.D., Lund, E.K., Loewen, M.A., Farke, A.A., and Clayton, K.E., 2013, A remarkable short-snouted horned dinosaur from the Late Cretaceous (late Campanian) of southern Laramidia: *Proceedings of the Royal Society B: Biological Sciences*, v. 280, no. 1766.

Sankey, J.T., 2008, Vertebrate paleoecology from microsites, Talley Mountain, upper Aguja Formation (Late Cretaceous), Big Bend National Park, Texas, in Sankey, J.T., and Baszio, S., eds., *Vertebrate Microfossil Assemblages: Their Role in Paleoecology and Paleobiogeography*: Bloomington, Indiana, Indiana University Press, p. 1–31.

Saupe, E.E., Hendricks, J.R., Portell, R.W., Dowsett, H.J., Haywood, A., and Hunter, S.J., 2014, Macroevolutionary consequences of profound climate change on niche evolution in marine molluscs over the past three million years: *Proceedings of the Royal Society B: Biological Sciences*, v. 281, no. 1795.

Scotese, C.R., and Wright, N., 2018, PALEOMAP paleodigital elevation models (PaleoDEMs) for the Phanerozoic: [https://www.earthbyte.org/webdav/ftp/Data\\_Collections/Scotese\\_Wright\\_2018\\_PaleoDEM/Scotese\\_Wright2018\\_PALEOMAP\\_PaleoDEMs.pdf](https://www.earthbyte.org/webdav/ftp/Data_Collections/Scotese_Wright_2018_PaleoDEM/Scotese_Wright2018_PALEOMAP_PaleoDEMs.pdf) (accessed December 2020).

Shepard, D., 1968, A two-dimensional interpolation function for irregularly-spaced data: *Proceedings of the 1968 23rd Association for Computing Machinery National Conference*, p. 517–524.

Sidor, C.A., O'Keefe, F.R., Damiani, R., Steyer, J.S., Smith, R.M.H., and Larsson, H.C.E., et al., 2005, Permian tetrapods from the Sahara show climate-controlled endemism in Pangaea: *Nature*, v. 434, p. 886–889, <https://doi.org/10.1038/nature03393>.

Sloan, R.E., 1970, Cretaceous and Paleocene terrestrial communities of western North America: *Proceedings of the North American Paleontological Convention*, Field Museum of Natural History, Chicago, September 5–7, 1969, 427–453.

Sloan, R.E., 1976, The ecology of dinosaur extinction, in Churcher, C.S., ed., *Essays on Palaeontology in Honour of Loris Shano Russell*: Toronto, Canada, Royal Ontario Museum, p. 134–154.

Steel, R.J., Plink-Bjorklund, P., and Aschoff, J., 2012, Tidal deposits of the Campanian Western Interior Seaway, Wyoming, Utah and Colorado, USA, in Davis, R.J., and Dalrymple, R., eds., *Principles of Tidal Sedimentology*: Heidelberg, Springer Netherlands, p. 437–471, [https://doi.org/10.1007/978-94-007-0123-6\\_17](https://doi.org/10.1007/978-94-007-0123-6_17).

Sullivan, R.M., and Lucas, S.G., 2006, The Kirtlandian land-vertebrate “age”—faunal composition, temporal position and biostratigraphic correlation in the nonmarine Upper Cretaceous of western North America: *New Mexico Museum of Natural History and Science Bulletin*, v. 36, p. 7–29.

Thomson, T.J., Irmis, R.B., and Loewen, M.A., 2013, First occurrence of a tyrannosaurid dinosaur from the Mesaverde Group (Neslen Formation) of Utah: Implications for Upper Campanian Laramidian biogeography: *Cretaceous Research*, v. 43, p. 70–79, <https://doi.org/10.1016/j.cretres.2013.02.006>.

Tiffney, B.H., 1992, The role of vertebrate herbivory in the evolution of land plants: *Palaeobotanist*, v. 41, p. 87–97.

Upchurch, G.R., Kiehl, J., Shields, C., Scherer, J., and Scotese, C., 2015, Latitudinal temperature gradients and high-latitude temperatures during the latest Cretaceous: Congruence of geologic data and climate models: *Geology*, v. 43, no. 8, p. 683–686, <https://doi.org/10.1130/G36802.1>.

Vajda, V., and Bercovici, A., 2014, The global vegetation pattern across the Cretaceous–Paleogene mass extinction interval: A template for other extinction events: *Global and Planetary Change*, v. 122, p. 29–49, <https://doi.org/10.1016/j.gloplacha.2014.07.014>.

Van Boskirk, M.C., 1998, *The flora of the Eagle Formation and its significance for Late Cretaceous floristic evolution* [Ph.D. dissertation]: New Haven, Connecticut, Yale University.

Vavrek, M.J., 2011, Fossil: Palaeoecological and palaeogeographical analysis tools: *Palaeontologia Electronica*, v. 14, no. 1.

Vavrek, M.J., and Larsson, H.C.E., 2010, Low beta diversity of Maastrichtian dinosaurs of North America: *Proceedings of the National Academy of Sciences of the United States of America*, v. 107, no. 18, p. 8265–8268, <https://doi.org/10.1073/pnas.0913645107>.

Weishampel, D.B., and Horner, J.R., 1987, Dinosaurs, habitat bottlenecks, and the St. Mary River Formation, in Currie, P.J., and Koster, E.H., eds., *Forth Symposium on Mesozoic Terrestrial Ecosystems*, Drumheller, August 10–14, 1987: Royal Tyrrell Museum of Palaeontology, p. 224–229.

Weishampel, D.B., and Norman, D.B., 1989, Vertebrate herbivory in the Mesozoic: Jaws, plants, and evolutionary metrics, in Farlow, J.O., *Paleobiology of the Dinosaurs: Geological Society of America Special Paper* 238, p. 87–101, <https://doi.org/10.1130/SPE238-p87>.

Wick, S.L., and Lehman, T.M., 2013, A new ceratopsian dinosaur from the Javelina Formation (Maastrichtian) of West Texas and implications for chasmosaurine phylogeny: *Naturwissenschaften*, v. 100, no. 7, p. 667–682, <https://doi.org/10.1007/s00114-013-1063-0>.

Williamson, T.E., 2000, Review of Hadrosauridae (Dinosauria, Ornithischia) from the San Juan Basin, New Mexico, in Lucas, S., and Heckert, A., eds., *Dinosaurs of New Mexico: New Mexico Museum of Natural History and Science Bulletin* 17, p. 191–214.

Wolfe, J.A., and Upchurch, G.R., 1987, North American nonmarine climates and vegetation during the Late Cretaceous: *Palaeogeography, Palaeoclimatology, Palaeoecology*, v. 61, p. 33–77, [https://doi.org/10.1016/0031-0182\(87\)90040-X](https://doi.org/10.1016/0031-0182(87)90040-X).

Wright, S., 1982, The shifting balance theory and macroevolution: *Annual Review of Genetics*, v. 16, p. 1–19, <https://doi.org/10.1146/annurev.ge.16.120182.000245>.

Zaffos, A., 2019, *Velociraptor: Fossil Analysis*: <https://cran.r-project.org/web/packages/velociraptor/index.html> (accessed December 2020).

Zhang, L., Hay, W.W., Wang, C., and Gu, X., 2019, The evolution of latitudinal temperature gradients from the latest Cretaceous through the Present: *Earth-Science Reviews*, v. 189, p. 147–158, <https://doi.org/10.1016/j.earscirev.2019.01.025>.

SCIENCE EDITOR: BRAD S. SINGER

ASSOCIATE EDITOR: CINZIA CERVATO

MANUSCRIPT RECEIVED 14 SEPTEMBER 2020

REVISED MANUSCRIPT RECEIVED 8 DECEMBER 2020

MANUSCRIPT ACCEPTED 21 DECEMBER 2020

Printed in the USA